MECHANISM FOR THE INSTABILITY OF SLOPES COMPOSED OF GRANULAR MATERIALS

YUICHI ONDA[1]* AND YUKINORI MATSUKURA[2]
[1] *Laboratory of Forest Hydrology & Erosion Control Engineering, School of Agricultural Sciences, Nagoya University, Nagoya 464-01, Japan*
[2] *Institute of Geoscience, University of Tsukuba, Tsukuba 305, Japan*

Received 16 March 1995; Revised 20 March 1996; Accepted 23 April 1996

ABSTRACT

The mechanism of instability of slopes composed of granular materials was examined through a tilting-box experiment using an assembly of aluminium rods and direct shear tests. A detailed observation of the experiment and the simple physical model led to the following conclusion. Avalanching of granular materials is triggered by rotation of rods at the slope surface. The force inducing the rotation was caused by the weight of the particles transmitted through contact points. Therefore, the mechanism of avalanching of granular materials was not comparable to the shear mechanism that has been considered to be responsible for the instability of slopes made of granular materials. © 1997 by John Wiley & Sons, Ltd.

Earth surf. processes landf., **22,** 401–411 (1997)
No. of figures: 11 No. of tables: 1 No. of refs: 25
KEY WORDS: slope stability; angle of repose; granular materials; shear strength; mechanism of avalanching

INTRODUCTION

Masses of discrete particles having no cementing matter at points of particle contact are called granular materials, and are an important component of the Earth's surface. Although studies on the mechanism of shear behaviour in materials are common in soil mechanics, little attention has been paid to the mechanism of avalanching on slopes made of granular materials. In the fields of sedimentology and geomorphology, some attempts have been made to examine this mechanism (e.g. Bagnold, 1954; Allen, 1970; Ishii, 1978). However, the mechanism remains unclear because of the difficulty of obtaining actual conditions during avalanching. Even in experiments conducted using equipment with a transparent side wall, the movement of individual particles that can be seen through the wall is influenced by friction between particles and the side wall (Carrigy, 1970).

To simplify three-dimensional phenomena of avalanching, a two-dimensional laboratory experiment was conducted using an assembly of aluminium rods to simulate a slope made of granular materials. The slope is made by piling up these rods. This kind of experiment has been proven to simulate the behaviour of granular assemblies well (e.g. Schneebeli, 1956; Dantu, 1957; Drescher and De Jong, 1972; Matsuoka, 1974). Since the experimental apparatus has no side walls, the movement of particles is not influenced by a wall effect.

To simulate the behaviour of granular materials, some models have been proposed, including a discrete element model (DEM), extended to two-dimensional disc elements by Cundall and Strack (1979). The DEM has recently been used to simulate the dynamic behaviour of particles during shear (e.g. Cundall and Strack, 1979; Ting *et al.*, 1988), dynamic liquefaction of sand (Tarumi and Hakuno, 1988), and dynamic fracture of soil (Iwashita, 1988). However, no studies have applied these models to the mechanism of avalanche initiation for granular materials.

When avalanches are initiated, the frictional resistance is assumed to be static. Therefore, the first step in solving the mechanism of avalanching is to examine static equilibrium of particles. A detailed observation of the two-dimensional avalanche is therefore conducted in this study. From the results of the experiments and a simple physical analysis, this paper attempts to investigate the mechanism of the stability of slopes composed of granular materials.

* Correspondence to: Y. Onda

CCC 0197-9337/97/040401–11 $17.50

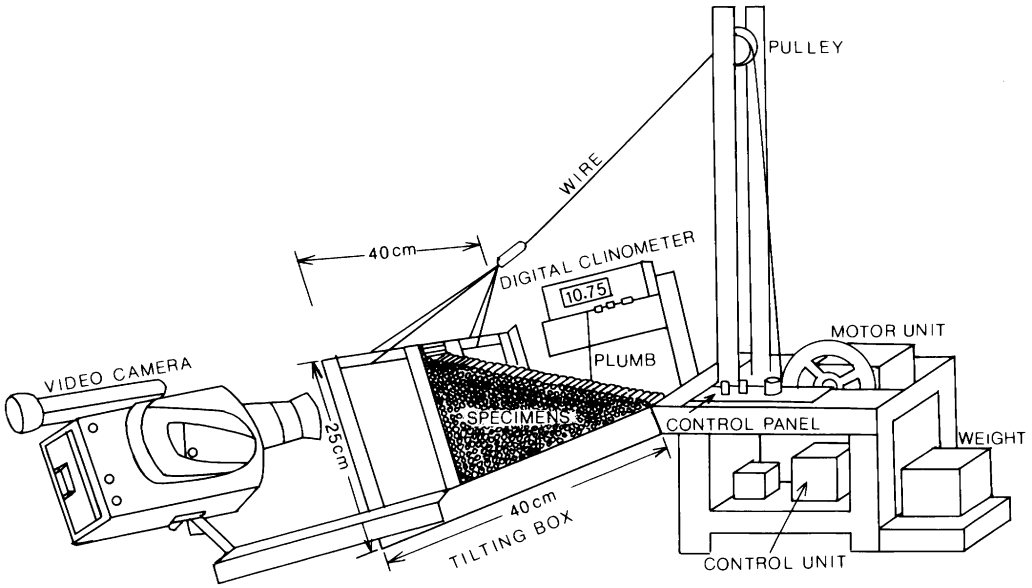

Figure 1. Diagram of the tilting-box apparatus

LABORATORY EXPERIMENTS

Experimental material, experimental apparatus and procedure

Aluminium rods with various cross-sections, all 50 mm in length, were employed in the present experiment. They were cylindrical, ellipsoidal, oval, square, rectangular and hexagonal in section. The cylindrical rods had four different diameters: 5, 9, 25 and 45 mm. Cylindrical rods of 5 mm and 8 mm diameter were pressed to make two kinds of ellipsoidal and oval rods: (a) those with an ellipsoidal cross-section with a long axis, a, of 5·7 mm and a short axis, b, of 4·2 mm, and a=9·1 mm, b=6·4 mm, respectively; and (b) those with an oval section with a=5·6 mm, b=3·9 mm, and a=8·7 mm, b=6·6 mm, respectively. Ellipsoidal and oval rods had cross-sectional shapes of an ellipse (as shown in Figure 2) and an athletic field (as shown in Figure 3), respectively. Square rods had sides of 5 mm, rectangular rods 6 and 9 mm, and hexagonal rods 4·5 mm.

A series of tests were conducted using a tilting box, consisting of a driving gear and a tilting L-shaped frame that was hinged on the driving gear (Figure 1). The L-shaped frame had a length of 40 cm, a height of 25 cm and a width of 40 cm and had no side walls. The bottom and the backboard of the frame were made of plastic plates, on to which a single layer of rods, identical to those used in each experiment, was glued.

The rods were piled up on the frame to make a wedge-shaped assembly as shown in Figure 1. The upper part of the frame was suspended by a wire, which was connected to a motor passing over a pulley at the top of a tower. The rod assembly was tilted by pulling the wire at a slow constant speed of 0·2° arc s^{-1} for the present experiment. The motion of rods was recorded by a 35 mm camera and a video camera operated at 30 frames s^{-1}.

The peak angle of shearing resistance, ϕ'_p, which is fundamental to slope stability analysis (Lambe and Whitman, 1979), was obtained through direct shear tests in this study. The aluminium rods were piled in a shear box up to 10 cm in height and they were sheared at a constant displacement rate of 1 mm min^{-1} under normal stresses ranging from 46 to 200 kPa.

Four kinds of rod arrangement were made (Figure 2): (A) regular packing, a close-packed hexagonal arrangement of monosized cylindrical rods; (B) random packing, using several kinds of rods; (C) horizontal packing, using ellipsoidal or oval rods with the direction of the long axis of rods being parallel to the slope; and (D) vertical packing, using ellipsoidal or oval rods with the direction of the long axis of rods being vertical to the bottom of the frame.

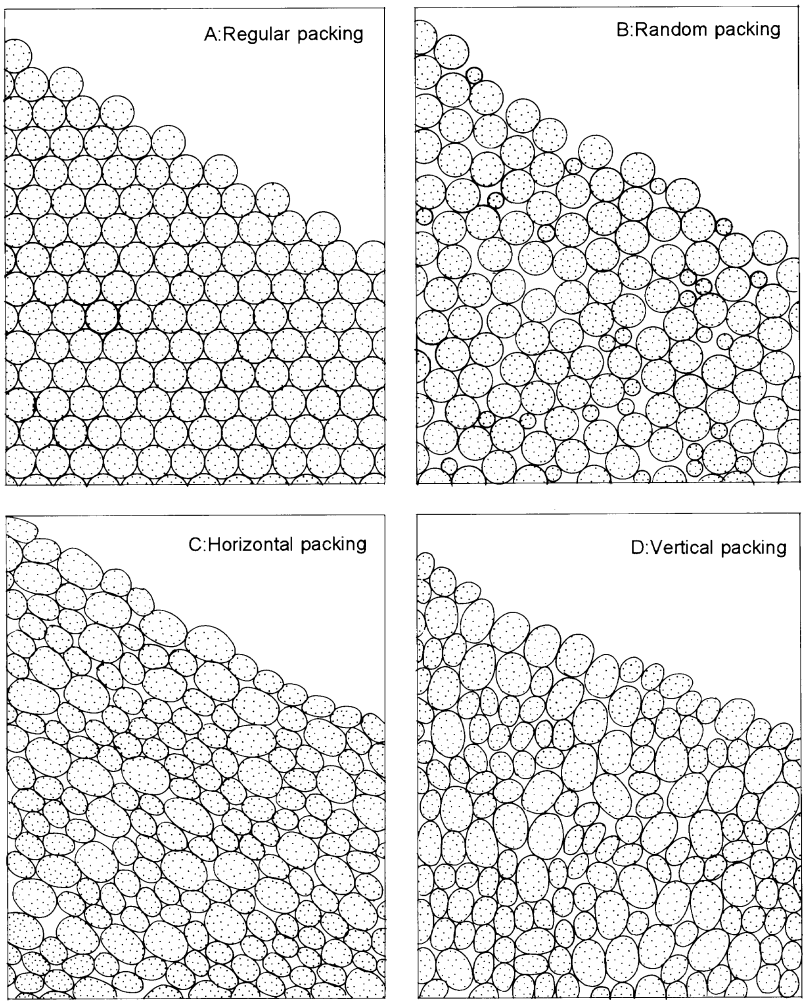

Figure 2. Schematic diagram of rod arrangements: (A) regular packing; (B) random packing; (C) horizontal packing; and (D) vertical packing

Mechanism of avalanching on the rod assembly

With increasing slope angle, some rods became unstable and started tumbling down the slope, while others remained stable. As the angle increased further, avalanching, involving all the rods near the surface of the slope, finally occurred. Figure 3 shows a typical example of the cross-section of an avalanche occurring on a slope made of oval rods with vertical packing. Observation of the video-taped images shows that the avalanche is like a flow of liquid; the amount of displacement of rods decreased with increasing depth from the avalanche surface. Onda *et al.* (1988) found that the behaviour of rods in the tilting-box experiment described above was similar to the avalanching of slopes made of sand or gravel.

To observe the initiation of avalanches, tilting-box experiments were made using a randomly packed mixture of rectangular, square and hexagonal rods (Figure 4). Although these rods were not round, avalanching was triggered by rolling. Figure 4b shows that two rods, a rod marked by an arrow and a rod below this, rotated first. Movement of these rods caused successive rotation of rods such as those marked A, B and D, which became unstable as their supports shifted, and an avalanche occurred. In short, the avalanche was triggered by rotation of the arrowed rod.

Figure 3. An avalanche occurred at the upper part of the slope using a mixture of larger and smaller oval rods with vertical packing (mixing ratio 3:2 by weight)

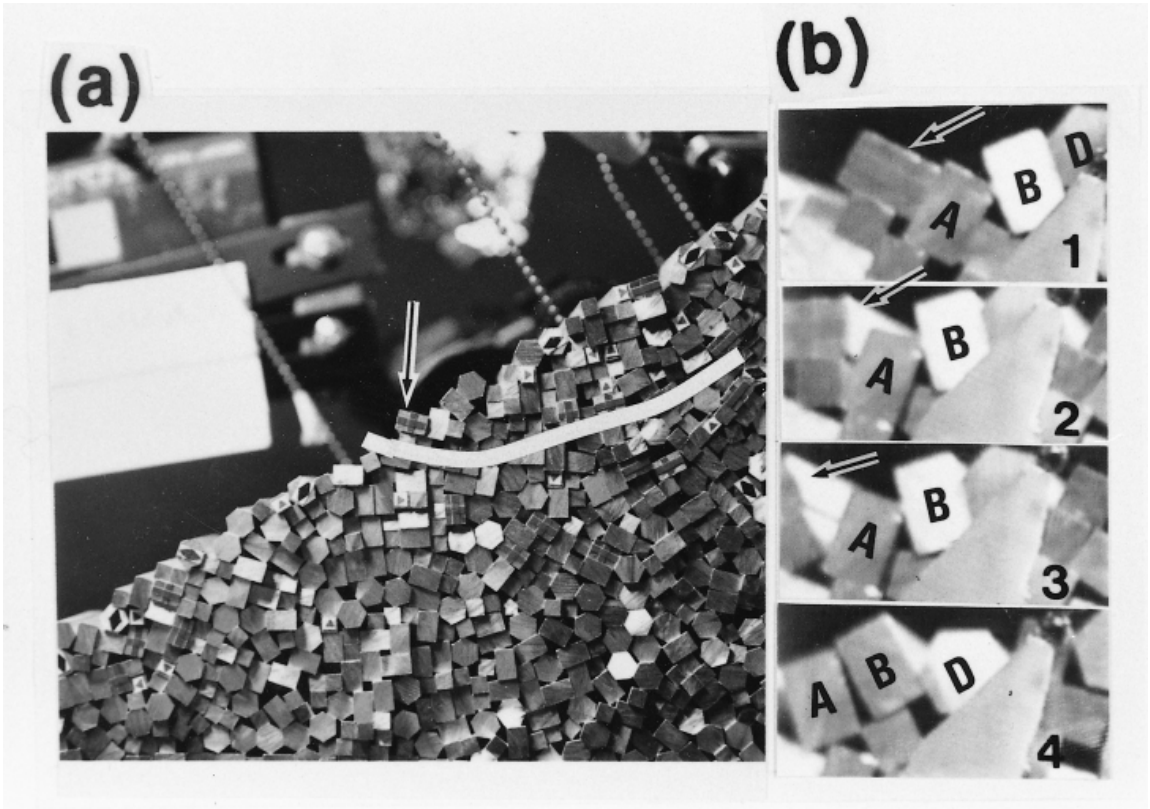

Figure 4. An avalanche in the case of a mixture of rectangular, square and hexagonal rods: (a) represents the state of packing – an avalanche occurs at the upper part of the white line; (b) indicates the commencement of avalanching taken with an interval of 1/30 s. The arrowed rod indicates the same rod in (a) and (b)

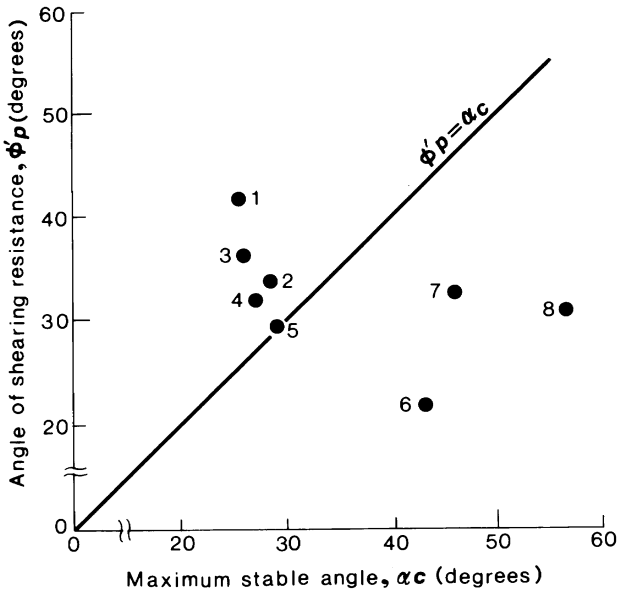

Figure 5. The maximum stable angle, α_c, versus the peak angle of shearing resistance, ϕ'_p. Data points numbered 1 and 2 are from Onda *et al.* (1989) who used a shear box 15 cm long, 10 cm wide and 10 cm deep. The other ϕ'_p values were obtained using a shear box 18 cm long, 10 cm wide and 10 cm deep. The numbered data points represent the various experimental cases. Case 1, mixture of smaller and larger ellipsoidal rods with vertical packing; ratio of mixture is 3:2 by weight (i.e. mixed ellipsoidal rods (3:2) with vertical packing). Case 2, mixed ellipsoidal rods (3:2) with horizontal packing. Case 3, mixed oval rods (3:2) with vertical packing. Case 4, mixed cylindrical rods (3:2) with random packing. Case 5, mixed oval rods with horizontal packing. Case 6, larger oval rods only wih horizontal packing. Case 7, larger oval rods only with vertical packing. Case 8, smaller cylindrical rods only with regular packing

Observations throughout the experiment suggested that avalanching was triggered by rolling of a single rod, resulting in the tumbling down of many distinct rods. The mechanism of avalanching of granular assemblies, therefore, cannot be analogous to the sliding of a solid body.

Measured value of the critical angle of repose and angle of shearing resistance

The maximum angle of slopes composed of granular materials is denoted as the critical angle of repose, α_c (e.g. Carrigy, 1970), and is referred to as the angle of avalanche commencement. The α_c values for assemblies of rods obtained from the tilting-box experiment versus the values for the peak angle of shearing resistance, ϕ'_p, with the same packing states (Onda *et al.*, 1989; Onda and Matsukura, 1991) is shown in Figure 5.

The solid line indicates where perfect agreement between α_c and ϕ'_p would be. The data plotted in Figure 5 are scattered, and correlation between the values is poor. The assembly of mixed ellipsoidal rods (case 2) and oval rods (case 5) with horizontal packing take on a higher α_c value and lower ϕ'_p value compared with vertically packed rods (cases 1 and 3). The α_c value for uniform-sized cylindrical rods with regular packing (case 8) is much higher than the other data; the α_c value is 56·5°, which is approximately 1·8 times as large as the ϕ'_p value. In other words, the α_c value depends greatly on whether the packing is regular or not, whereas the ϕ'_p value does not. This fact also indicates that the instability of slopes composed of granular materials is not regulated by the angle of shearing resistance.

ANALYSIS OF ROD MOVEMENT

Friction of individual aluminium rods

The primary parameter for static behaviour of many particles is the angle of friction between particles (Rowe, 1962). There are two kinds of friction, rolling friction (Figure 6a) and sliding friction (Figure 6b). As

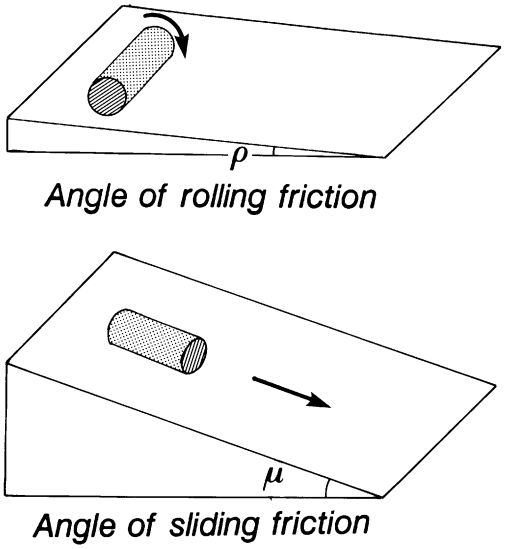

Figure 6. Measuring methods for (a) angle of rolling friction, ρ, and (b) angle of sliding friction, μ

described before, particle rolling is of vital importance at the initiation of an avalanche. Therefore, rolling as well as sliding friction of individual rods should be evaluated for analysing the stability of slopes.

To determine the value of the friction angle of the aluminium rods used in this study, tests were performed using the tilting box, in which a rod was placed on a slope made of aluminium plate (Figure 6). The value for the angle of sliding friction, μ, was measured as the angle at which the rod just starts sliding when aligned parallel to the slope direction (Figure 6b). This value corresponds to the particle-to-particle sliding friction, ϕ_m (Rowe, 1962). The tests were repeated 100 times and the average value of μ was obtained.

Frictional resistance is assumed to be very small when cylinders roll without slipping. The angle of rolling friction was measured as the angle at which a rod, placed perpendicularr to the slope direction, just started rolling. The equilibrium in the critical condition for rolling is expressed as:

$$M_i = \boldsymbol{F} r \tag{1}$$

where M_i is the rolling moment resisting rotation, $\boldsymbol{F}$ is the force applied to the rod, equivalent to the downslope component of the mass of the rod, and r is the radius of the rod, corresponding to the length of the arm of the moment. The resisting moment, M_i, can be rewritten as:

$$M_i = Wr \sin \rho \tag{2}$$

where W is the weight of the rod and ρ is the angle at which the rod just starts rolling. This angle is defined as the angle of rolling friction in this study (Figure 6a). The tests were made for various rod diameters and were repeated 100 times for each case, and the average value of ρ was obtained.

The test results are listed in Table I. The values of rolling friction were much smaller than those of the sliding friction: taking 9 mm rods as an example, ρ and μ are 1·37° and 19·8, respectively. The value of ρ decreases with increasing diameter of rods (Bikerman, 1949).

Table I. Sliding friction angle (in degrees) and rolling friction angle of an aluminium rod

Diameter (mm)	Sliding friction, μ	Rolling friction, ρ
5	19·8	2·21
9	19·8	1·37
25	19·8	0·92
45	19·8	0·50

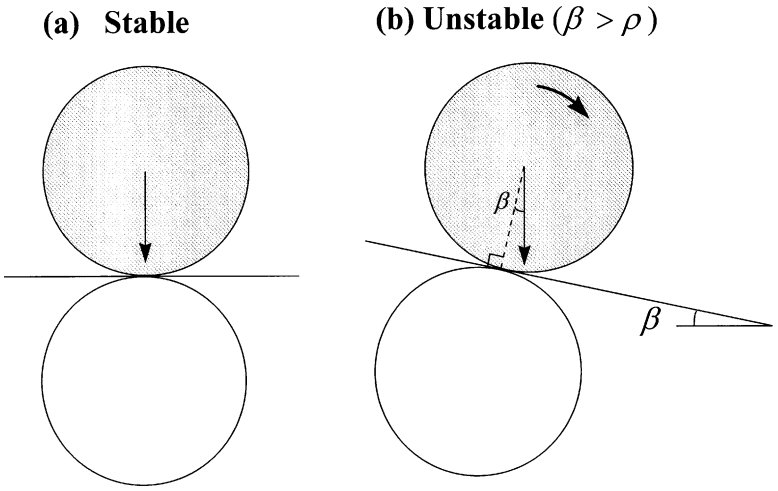

Figure 7. Critical condition of movement between two rods: (a) stable, (b) unstable

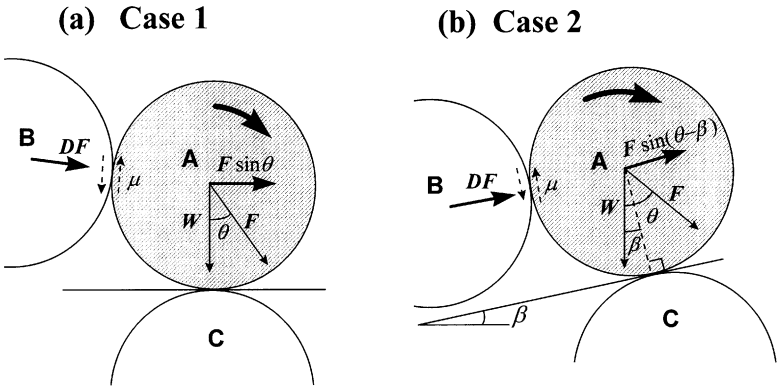

Figure 8. Critical condition of movement between two rods for the case in which one rod is pushed by another rod: (a) tangential line between A and C is horizontal; (b) tangential line between A and C is not horizontal

Critical condition of the rod movement in a mass of rods

A simple case of the critical condition of rod movement in a mass of rods is a balance between two rods. It would be reasonable to assume that a tangential line between rods is identical to the slope situation. Therefore, a critical condition between two rods is described in Figure 7; if the angle of the tangential line between two rods (β) is lower than the angle of rolling friction, the rods tend to be stable, and at $\beta>\rho$ the rod will begin rolling.

The next case is that one rod is pushed by another rod. As depicted in Figure 8a, a total force $\boldsymbol{F}$ of rod A has a direction with an angle of θ from the horizontal plane, because rod A is pushed by rod B. In this case, the tangential line between two rods is assumed to be horizontal. When rod A starts rolling on rod B, sliding should take place at the boundary between rods A and B; as a result, the effective movement of rotation would decrease. Here, the moment causing a rod movement, M_r, is calculated as:

$$M_r = \boldsymbol{F} \sin\theta r \tag{3}$$

and resisting moment, M_i, is:

$$M_i = (W \sin\rho + \mu \boldsymbol{DF}) r \tag{4}$$

Therefore, the critical condition for rod movement, M_c is:

$$M_c = (\boldsymbol{F} \sin\theta - W \sin\rho - \mu \boldsymbol{DF}) r = 0 \tag{5}$$

(a)

(b)

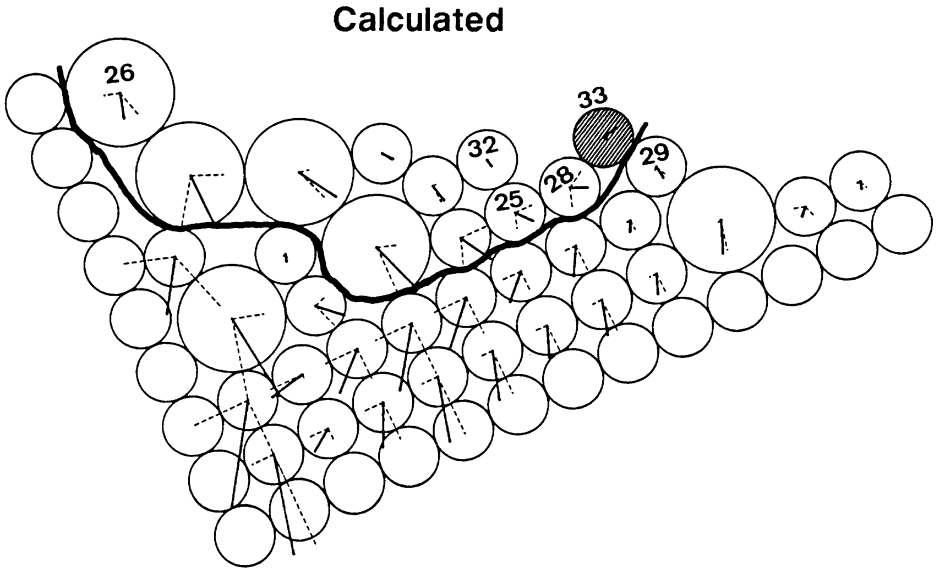

Figure 9. Typical examples of (a) the experiment with 35 rods, and (b) the numerical result at an angle of 13°

The next step is the more general situation that β is not assumed to be horizontal (Figure 8b). Where rod A starts moving, the rod with a weight of W should climb the slope with an angle of β. From the equilibrium of forces, the following equation is derived:

$$M_c = (\boldsymbol{F} \sin(\theta - \beta) - W \sin\beta - W \cos\theta \sin\rho - \mu \boldsymbol{DF}) r = 0 \quad (6)$$

Equations 5 and 6 express the critical condition for rod movement.

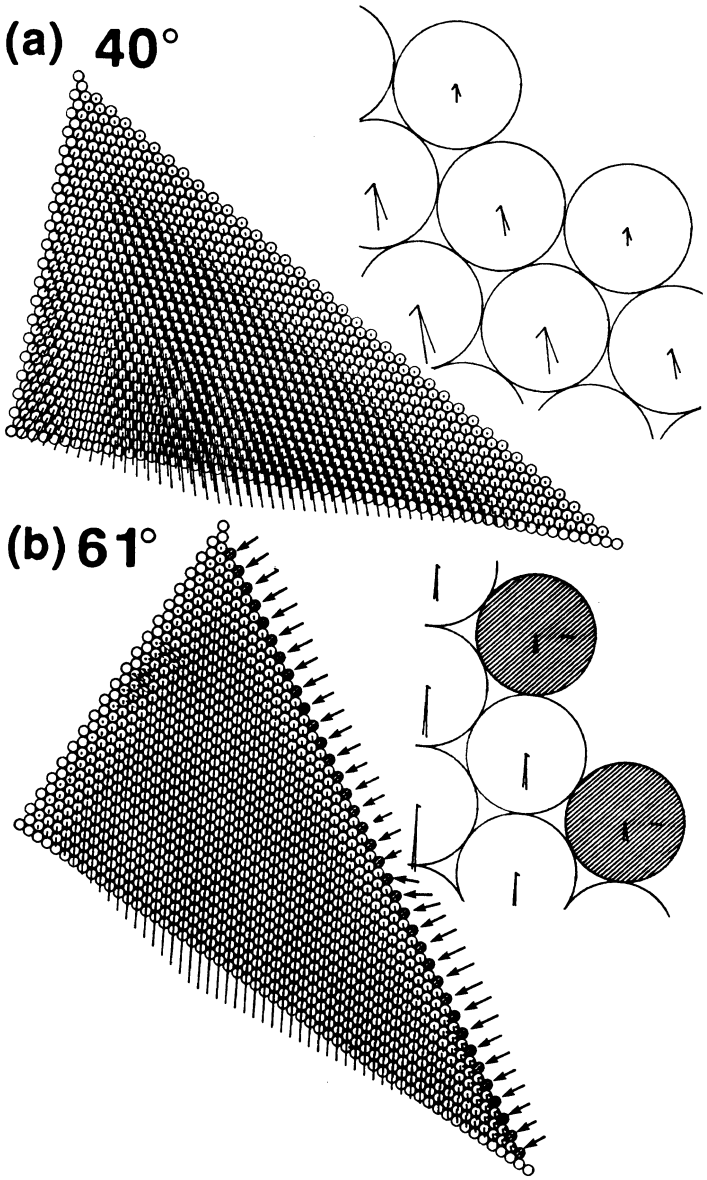

Figure 10. The results of numerical analysis in the case of uniform discs with regular packing: (a) 40°; (b) 61°. Shaded discs indicate the unstable discs

DISCUSSION AND CONCLUSIONS

Comparison between the static model and laboratory experiment

To test the validity of the static model, comparison between the numerical analysis and the laboratory experiment was made. Two kinds of discs simulated the cylindrical rods with diameters of 25 and 45 mm, respectively, the number of the former discs being 29 and that of the latter 6. The values μ and ρ, listed in Table I, were used in the physical analysis.

The analyses of internal force balance between rods employed a GSM (Onda, 1992), a simple static balance model for granular materials. The numerical calculation was executed by 1° steps in each case. The angle at

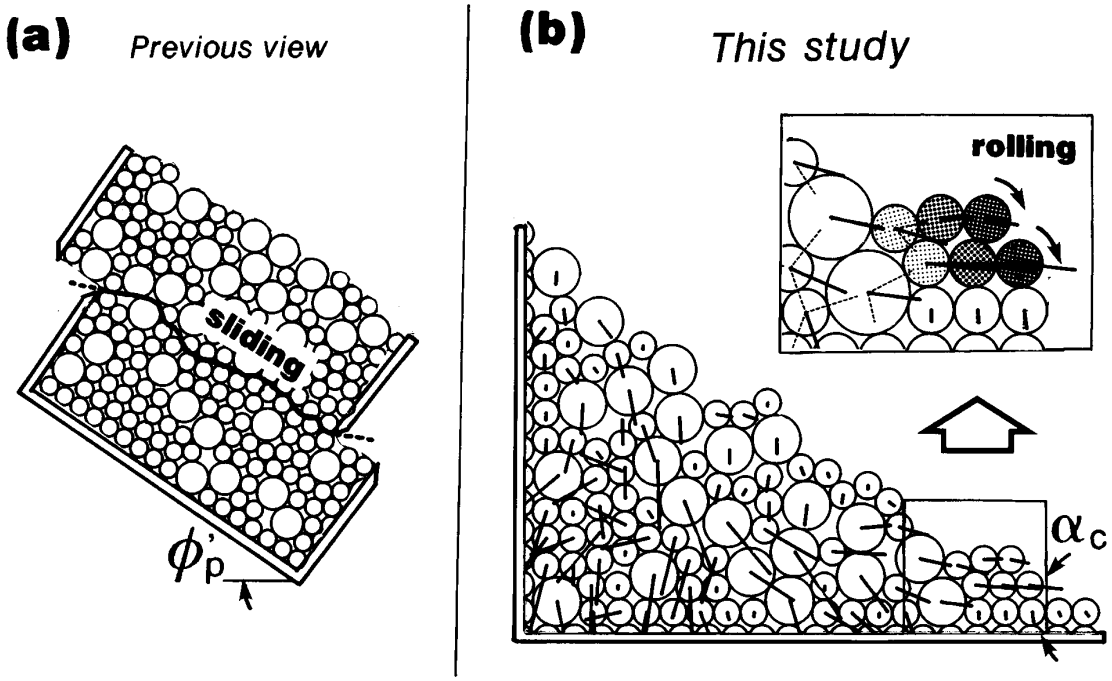

Figure 11. Schematic diagram showing the mechanism for avalanching: (a) previous views and (b) the view proposed in this paper

which a disc first started moving was recorded and denoted as α_m. In addition, judgement was made of which discs became unstable. The critical condition was calculated using Equation 6.

Figure 9 is a typical example of the experiment and the numerical result, where disc no. 33 was calculated to be unstable at an angle of 13·0°, i.e. $\alpha_m = 13{\cdot}0°$, even with a very high angle of the tangential line (β) between discs no. 33 and no. 29. In the experiment, rod no. 33 started rolling at 13·8°, and after that some other rods moved, i.e. those bordered by a white line in Figure 9a, such as rods nos. 28, 25 and 32. Inspection of the numerical result (Figure 9b) suggests that these rods moved because they were in balance with rod no. 33; these rods lost their balance as a result of missing their supports successively.

This static model was applied for the case of regular packing. All the discs are stable when the angle is 40° (Figure 10a). The directions of total forces of many discs at these angles are vertical, and particles support each other. At an angle of 61°, discs located at the surface became unstable, as shown in Figure 10b. This angle is close to the α_c value of 56·5° obtained through the tilting-box experiment (case 8 in Figure 5).

These results are the best explanation for α_c values being attributable to their packing states. This suggests that the slope instability is due to the imbalance of total forces caused by irregular arrangement of rods.

Critical angle of repose and angle of shearing resistance

The oldest and simplest procedure for obtaining the friction angle of dry granular soil is to observe the angle of small pile of the material (Taylor, 1948). It has been considered, therefore, that the avalanching of granular materials is analogous to the sliding of a solid body (e.g. Terzaghi, 1925; Seed and Goodman, 1969; Barton and Kjærnsli, 1981) and the angles at which avalanches take place are identified by the angle of shearing resistance of these materials, as illustrated in Figure 11a.

The present experiment clearly indicates that the mechanism controlling instability of slopes composed of granular assemblies is not comparable to the angle of shearing resistance (Onda and Matsukura, 1991; 1993; Caine, 1993), but mainly triggered by rolling on the slope surface. This fact strongly suggests that interparticle sliding friction, which has been thought to be the dominant shear mechanism, is not an important factor for the instability of slopes composed of granular materials.

Figure 11b is a schematic diagram showing the mechanism for avalanching of granular materials, which is elucidated from the present study. An avalanche is triggered by rolling of a rod on the surface. That movement results in loss of support to other rods, which leads to the successive occurrence of rolling; i.e. an avalanche occurs. This shows a strong contrast to the shearing mechanism, which has previously been considered to be responsible for the instability of slopes made of granular materials.

ACKNOWLEDGEMENTS

Thanks are due to Professor Tsuguo Sunamura, Institute of Geoscience, University of Tsukuba, who reviewed the manuscript and gave useful suggestions.

REFERENCES

Allen, J. R. L. 1970. 'The avalanching of granular solids on dune and similar slopes', *Journal of Geology*, **78**, 326–351.

Bagnold, F. R. S. 1954. 'Experiment on a gravity-free dispersion of large solid spheres in a Newtonian fluid under shear', *Proceedings of the Royal Society*, **A225**, 49–63.

Barton, N. and Kjærnsli, B. 1981. 'Shear strength of rockfill', *Proceedings of the American Society of Civil Engineering*, **107**(GT7), 873–891.

Bikerman, J. J. 1949. 'Effect of surface roughness on rolling friction', *Journal of Applied Physics*, **20**, 971–975.

Caine, N. 1993. 'Is the maximum stable angle of slope of granular assemblies comparable to the angle of shearing resistance?: A comment', *Transactions, Japanese Geomorphological Union*, **14**, 423–425.

Carrigy, M. A. 1970. 'Experiments on the angles of repose of granular materials', *Sedimentology*, **14**, 147–158.

Cundall, P. A. and Strack, O. D. L. 1979. 'A discrete numerical model for granular assemblies', *Géotechnique*, **29**, 47–65.

Dantu, P. 1957. 'A contribution to the mechanical and geometrical study of non-cohesive masses', *Proceedings of the 4th International Conference of the Soil Mechanics and Foundation Engineering*, 144–148 (in French with English abstract).

Drescher, A. and De Jong, G. D. J. 1972. 'Photoelastic verification of a mechanical model for the flow of granular material', *Journal of the Mechanics and Physics of Solids*, **20**, 337–351.

Ishii, T. 1978. 'Influences of the grain size of rock fragment and the slope length on the development of talus slope', *Geographical Report of Osaka Kyoiku University*, **17**, 35–46.

Iwashita, K. 1988. 'Dynamic fracture analysis of ground by granular assembly simulation I', *Bulletin of the Earthquake Research Institute, University of Tokyo*, **63**, 201–235 (in Japanese with English abstract).

Lambe, T. W. and Whitman, R. V. 1979. *Soil Mechanics SI version*, Wiley, New York, pp. 192–193.

Matsuoka, H. 1974. 'A macroscopic study on shear mechanism of granular materials', *Soils and Foundations*, **14**(1), 29–43.

Onda, Y. 1992. 'A model on the stability of slopes composed of granular materials', *Science Report, Institute of Geoscience, University of Tsukuba*, Sect. A, **12**, 13–34.

Onda, Y. and Matsukura, Y. 1991. 'Is the maximum stable angle of slope of granular assemblies comparable to the angle of shearing resistance?', *Transactions, Japanese Geomorphological Union*, **12**, 147–154.

Onda, Y. and Matsukura, Y. 1993. 'A reply to the preceding comment by Nel Caine on 'Is the maximum stable angle of slope of granular assemblies comparable to the angle of shearing resistance?', *Transactions, Japanese Geomorphological Union*, **14**, 427–429.

Onda, Y., Matsukura, Y., Iseki, H. and Okuyama, T. 1988. 'Preliminary study on angle of initial yield and angle of rest by tilting-box tests', *Bulletin of the Environmental Research Centre, University of Tsukuba*, **12**, 49–55 (in Japanese).

Onda, Y., Matsukura, Y., Matsuoka, H. and Oh-hashi, H. 1989. 'A preliminary study on failure mechanism of slope composed of two-dimensional granular materials, *Proceedings of the 24th Japanese Conference of Soil Mechanics and Foundation Engineering*, 1605–1606 (in Japanese).

Rowe, P. W. 1962. 'The stress–dilatancy relation for static equilibrium of an assembly of particles in contact', *Proceedings of the Royal Society*, **A269**, 500–527.

Schneebeli, M. G. 1956. 'Mécanique des soils – Une analogie mécanique pour les terres sans cohésion', *Comptes Rendes Hebdomaires des Seances de l'Academie des Sciences*, **243**, 125–126 (in French).

Seed, B. and Goodman, R. E. 1964. 'Earthquake stability of slopes of cohesionless soils', *Proceedings of the American Society of Civil Engineering*, **90**(SM6), 43–73.

Tarumi, Y. and Hakuno, M. 1988. 'A granular assembly simulation for the dynamic liquefaction of sand', *Natural Disaster Science*, **10**, 45–59.

Taylor, L. D. W. 1948. *Fundamentals of Soil Mechanics*, Wiley, New York, 345–351.

Terzaghi, C. 1925. 'Principles of soil mechanics (2): Friction in sand and clay', *Engineering News Record*, **95**, 1026–1029.

Ting, J. M., Corkum, B. T., Kauffman, C. R. and Greco, C. 1989. 'Discrete numerical model for soil mechanics', *Proceedings of the American Society of Civil Engineering*, **115**(GT3), 379–398.